Aquaporins are main contributors of root hydraulic conductivity in pearl millet [*Pennisetum glaucum* (L) R. Br.]

Alexandre Grondin[1,2,3,4*], Pablo Affortit[1,2], Christine Tranchant-Dubreuil[1], Carla de la Fuente Cantó[1], Cédric Mariac[1], Pascal Gantet[1], Vincent Vadez[1,5], Yves Vigouroux[1], Laurent Laplaze[1,2]

[1] UMR DIADE, IRD, Université de Montpellier, Montpellier, France

[2] Laboratoire mixte international Adaptation des Plantes et microorganismes associés aux Stress Environnementaux, Dakar, Senegal

[3] Laboratoire Commun de Microbiologie, Dakar, Senegal

[4] Centre d'Etude Régional pour l'Amélioration de l'Adaptation à la Sécheresse, Thiès, Senegal

[5] International Crops Research Institute for Semi-Arid Tropics (ICRISAT), Patancheru, India

* Corresponding author

E-mail: alexandre.grondin@ird.fr

Abstract

Pearl millet is a key cereal for food security in arid and semi-arid regions but its yield is increasingly threatened by water stress. Physiological mechanisms consisting in saving water or increasing water use efficiency can alleviate that stress. Aquaporins (AQP) are water channels contributing to plant hydraulic balance that are supposedly involved in these mechanisms by mediating root water transport. However, AQP remain largely uncharacterized in pearl millet. Here, we studied AQP function in root water transport in two pearl millet lines contrasting for water use efficiency (WUE). We observed that these lines were also contrasting for root hydraulic conductivity (Lpr) and AQP contribution to Lpr, the line with lower WUE showing significantly higher AQP contribution to Lpr. To investigate the AQP isoforms contributing to Lpr, we developed genomic approaches to first identify the entire AQP family in pearl millet and second study the plasma membrane intrinsic proteins (PIP) gene expression profile. We identified and annotated 33 AQP genes in pearl millet among which ten encoded PIP isoforms. *PgPIP1-3* and *PgPIP1-4* were significantly more expressed in the line showing lower WUE, higher Lpr and higher AQP contribution to Lpr. Overall, our study suggests that AQP from the PIP1 family are the main contributor of Lpr in pearl millet and are possibly associated to whole plant water use mechanisms. This study paves the way for further investigations on AQP functions in pearl millet hydraulics and adaptation to environmental stresses.

Key-words: pearl millet, aquaporin, water, roots.

The newly sequenced nucleotide sequences reported in this article have been submitted to GenBank under the submission number 2333840 (TPA grp467567). Assignment of GenBank accession number is in process.

Introduction

Plant hydraulics depends on soil water capture by roots, transport to the leaves and diffusion as vapor from the stomatal cavity to the atmosphere. In this plant hydraulic continuum, the radial water transport from the soil solution to the xylem vessels uses two paths: the apoplastic path where water can flow along the cell wall structures, and the cell to cell path where water can flow across cell membranes (transcellular) or along cytoplasmic continuities formed by plasmodesmata (symplastic) [1]. Extracellular hydrophobic barriers of lignin and suberin located in the endodermis are thought to restrict diffusion of water along the apoplastic path [2]. In the presence of such barriers, the cell to cell path is favored by water channels present in cell membranes called aquaporins [3].

Aquaporins (AQP) are present throughout the living kingdom at the exception of thermophilic Archaea and intracellular bacteria [4]. They belong to the Major Intrinsic Proteins (MIP) superfamily and are characterized by six transmembrane domains and two highly conserved Asn-Pro-Ala (NPA) motifs [5]. Other typical signatures of AQP consist in selectivity filters domains structuring the pore and composed of the aromatic/arginine (ar/R) motifs and the Froger's residues [6,7]. In higher plants, AQP isoforms fall into five families comprising the Plasma membrane Intrinsic Proteins (PIP), the Tonoplast Intrinsic Proteins (TIP), the Nodulin26-like Intrinsic Proteins (NIP), the Small Intrinsic Proteins (SIP) and the uncharacterized (X) Intrinsic Proteins (XIP) [8]. Although plant AQP have been localized throughout the cell secretory system, PIP, NIP and XIP are preferential residents of the plasma membranes while TIP accumulate in the tonoplast and SIP in the endoplasmic reticulum [9–11]. Functional studies combined with modelling approaches demonstrated that, more than being permeable to water, AQP possess a wide range of selectivity profiles [12,13]. Some PIP

73 isoforms are thereby permeable to H_2O_2 and CO_2, some TIP isoforms to NH_3 and urea, and
74 some NIP to small organic solutes or mineral nutrients [14–18]. AQP possess wide range of
75 physiological functions and have now been identified in a number of crop species such as rice,
76 maize, tomato, cotton, sorghum, *Setaria italica*, watermelon or *Cannabis sativa* [19–24].
77 In plants, AQP are involved in water transport in both roots and shoots. In Arabidopsis
78 for instance, isoforms AtPIP2-2 and AtPIP1-2 contributes to around 14% and 20% of the root
79 osmotic conductivity and shoot hydraulic conductivity, respectively [25,26]. AQP also have
80 important roles in plant growth, CO_2 fixation, nutrient allocation, reproduction or biotic
81 interactions [8]. In recent years, AQP functions in plant water relations have received more
82 attention as a potential target for crop improvement, particularly to increase tolerance to
83 drought [27–32]. For instance, AQP could regulate root water transport in order to match
84 transpiration and therefore contribute to mitigate disparity between water supply and
85 demand in soybean upon “atmospheric” water stress caused by high evaporative demand
86 [33]. This assumption is supported by the increased AQP expression and root hydraulic
87 conductivity upon transpiration demand in rice and grapevine [34,35]. Furthermore,
88 overexpression of *SiTIP2-2* in tomato increased transpiration rate and was associated with
89 improved fruit yield upon moderate soil water stress [36]. Conversely, in other crops more
90 adapted to hot and dry climates such as pearl millet, lower transpiration under high vapor
91 pressure deficit (VPD) has been proposed to be beneficial for tolerance to “atmospheric”
92 water stress and potentially associated with AQP function in root hydraulics [30,37,38].
93 Therefore, AQP may be involved in different physiological mechanisms that determine the
94 extent of water usage by the plant [39]. In fact, specific isoforms might be involved in different
95 scenarios, calling for a better understanding of AQP family members and their functions in
96 crops [28].

Pearl millet [*Pennisetum glaucum* (L) R Br.] is a key cereal for food security in arid and semi-arid regions [40]. However, its yield remain low and is often affected by climate unpredictability (heat waves and dry spells) that are forecast to worsen in future climate change scenarios [41,42]. The recent release of the pearl millet genome has opened new ways for functional genomic-based efforts aiming at improving its yield and tolerance to abiotic stresses [43]. In this study, we evaluated the potential links between AQP function in roots and water use, a drought tolerance-related trait, by measuring AQP contribution to Lpr and AQP genes expression in the roots of two pearl millet inbred lines contrasting for water use efficiency. To have more insights into the AQP isoforms contributing to root hydraulics, we characterized the entire AQP family in pearl millet using a genomic approach.

Materials and methods

Plant material and growth conditions

IP4952 and IP17150, two pearl millet inbred lines that are part of the Pearl Millet inbred Germplasm Association Panel (PMiGAP) were used in this study [43]. The water use efficiency of these two lines was characterized across two lysimeters experiments performed under well-irrigated conditions at the International Crops Research Institute for the Semi-Arid Tropics (ICRISAT, India) according to [44]. These experiments indicated that IP4952 and IP17150 displayed relatively low and high water use efficiency, respectively (2.35 versus 3.72) [45] These two lines were used for root hydraulic conductivity measurements and AQP expression analyses in which plant were grown in hydroponic conditions into a nethouse at the IRD/ISRA Bel Air research station (Dakar, Senegal; 14.701615 N – 17.425359 W). Plants were germinated in Petri dishes into a chamber at 37°C for two days in the dark. Plants were

120 further exposed to light (37°C, 12h day/night cycle) for one day before being transplanted on
121 top of a black mat covering a 30L container (45x40x24 cm containing 40 plants in total) filled
122 with half strength Hoagland solution [46]. The system allowed roots to strictly develop in the
123 nutrient solution without been exposed to light. Oxygen was provided to the roots through
124 constant bubbling of the solution using an air pump.
125

126 Root hydraulic conductivity and aquaporin contribution

127 Root hydraulic conductivity (Lpr) was measured in April-Mai 2019 (17/34°C and 34/100% in
128 minimum/maximum temperature and humidity, respectively) from 9AM to 12PM on 15 days
129 old plants grown in hydroponic conditions. The average temperature, relative humidity and
130 VDP at the time of measurements were 24.4 ± 0.3°C , 75.1 ± 1.2% and 0.8 ± 0.1, respectively.
131 Plants were grown sequentially to be analyzed at the same age in a randomized design taking
132 into account the time of measurement. Lpr measurements were performed using a pressure
133 bomb (model 1000, PMS instrument company, USA) according to [47] and [48]. Briefly, plants
134 were inserted into the pressure chamber filled with nutrient solution complemented or not
135 by 2mM of azide (NaN_3). The hypocotyl was carefully threated through the silicone grommet
136 of the pressure chamber lid while the intact root system was sealed into the chamber. Roots
137 were pressurized with compressed air at 0.4 MPa for 5 min to equilibrate, followed by xylem
138 sap collection at 0.1, 0.2 and 0.3 MPa for 5 min using pre-weighed 2 ml Eppendorf tubes filled
139 with cotton placed on top of the stem. The mass of xylem sap exuded at each pressure was
140 determined by weighing and used to calculate the xylem sap flow (slope of xylem sap weight
141 at each pressure). After the measurements, roots systems were scanned to determine root
142 surface area using WhinRhizo Pro version 2012b (Regent Instruments, Canada). Xylem sap flux

was divided by root surface area to calculate Lpr. AQP contribution to Lpr was estimated using relative Lpr inhibition by azide calculated as:

$$100 - ((Lpr_{azide\_individual\_replicate} \times 100) / Lpr_{no\_azide\_variety\_mean}) \quad (1)$$

Aquaporins genome-wide identification

A total of 772 AQP protein sequences from 19 plant species (*Arabidopsis thaliana, Beta vulgaris, Brachypodium distachyon, Cicer arietinum, Gossypium hirsutum, Glycine max, Hordeum vulgare, Linum usitatissimum, Musa acuminate, Panicum virgatum, Pennisetum glaucum, Populus tremula, Oryza sativa, Setaria italica, Solanum lycopersicum, Solanum tuberosum, Sorghum bicolor, Vitis vinifera* and *Zea mays*) were aligned against the pearl millet genome (ASM217483v2) and the non-assembled scaffolds [43] using tblastn with an e-value of 10^{-5} as initial cut-off to identify high scoring pairs. High scoring pairs were further filtered to keep those with a bit score ≥100. Hot-spots of high scoring pairs were identified and redundant high scoring pairs were filtered to keep those with highest bit-score for further analysis (S2 Table). The filtered high scoring pairs locations in the pearl millet genome were used to identify regions with homologies to AQP genes.

Structural annotation

Correspondence between selected high scoring pairs and annotated genes in the pearl millet genome was determined. Potential AQP genes were identified and their genomic sequence ± 1000pb upstream and downstream of the start/end position was retrieved as well as the predicted gene structure [43]. When predicted AQP did not correspond to previously annotated genes, the GENSCAN Web Server (http://hollywood.mit.edu/GENSCAN.html) was

166 used to predict the exon-intron structure of the genomic region. Putative AQP genomic
167 sequences were aligned against the Plant EST (downloaded in August 2018) and the
168 UniProt/Swiss-Prot plant protein (February 2016) databases and manually annotated using
169 the Artemis software (version 17.0.1, Sanger Institute, UK; S3 Table). Annotation was
170 confirmed by aligning reads from pearl millet transcriptomes [49] on the pearl millet genome
171 using the Tablet software (version 1.19.09.03) [50] and coding and protein sequences were
172 generated. AQP gene structure were further visualized using GSDS2.0 software [51].
173

174 ## Sequencing

175 AQP genes sowing missing sequences in or bordering coding regions were resequenced (S3
176 Table) using genomic DNA or cDNA from Tift 23D2B1 (genotype used to draft the pearl millet
177 whole genome sequence). DNA was prepared using DNeasy Plant mini extraction kit (Qiagen,
178 Germany) while cDNA was prepared by first extracting RNA using the RNeasy Plant mini
179 extraction kit (Qiagen, Germany) followed by DNAse treatment (RNase-free DNase set;
180 Qiagen, Germany) and reverse transcription reaction (Omniscript RT kit; Qiagen, Germany)
181 according to the manufacturer's instructions. Corresponding DNA/cDNA fragments were
182 amplified using the Phusion high-fidelity DNA polymerase (Thermo Scientific, USA), purified
183 (Geneclean turbo kit, MP Biomedicals, USA) and sent for sequencing (Eurofins Genomics,
184 Germany). Primers used for amplification are presented in S4 Table. Difficulties in amplifying
185 the missing sequence of PgTIP5-1 were encountered. In that specific case, we used
186 unpublished MINION reads (Mariac, Vigouroux, Berthouly-Salazar; unpublished) to complete
187 its sequence. Missing nucleotides were added to the pearl millet genomic sequence and
188 coding frame of the corresponding new protein was carefully checked.
189

Identification of functional motifs and transmembrane domains

The NCBI conserved domain database (CDD) was used to identify NPA motifs and aromatic/arginine (ar/R) selectivity filters in the putative AQP protein sequences. Froger's residues were identified according to [6]. The number and location of the transmembrane domains were studied using TMHMM (http://www.cbs.dtu.dk/services/TMHMM/), TMpred (https://embnet.vital-it.ch/software/TMPRED_form.html) and Phyre2 [52]. Protein sequences were aligned using the CLUSTALW alignment function in the Maga7 software (version 7.0.26) [53]. Alignments were colored using the Color Align Properties program (https://www.bioinformatics.org/sms2/color_align_prop.html). Conserved domains as well as transmembrane domains were further manually analyzed to detect sequence alterations. Three-dimensional geometry structure and pore morphology of PIP was obtained using the PoreWalker software (https://www.ebi.ac.uk/thornton-srv/software/PoreWalker/).

Phylogenetic analysis

Phylogenetic analyses of *P. glaucum* AQP (PgAQP) was analyzed in relation to AQP identified in *A. thaliana* (AtAQP), *O. sativa* (OsAQP) and *P. tremula* (PtAQP) using the Mega7 software (version 7.0.26) [53]. PgAQP, AtAQP, OsAQP and PtAQP protein sequences were aligned using the CLUSTAW function and phylogenetic tree was built using the maximum likelihood method with 1000 reiterations. This allowed determination of the statistical stability of each node. Based on their position in the phylogenetic tree, PgAQP isoforms were classified into PIP, SIP, TIP and NIP families and named according to their close homologs.

Expression profiling

P. glaucum PIP (PgPIP) genes expression were measured in root of 15 days old plants grown in hydroponic conditions using quantitative polymerase chain reaction (RT-PCR). Roots (seminal + one crown root) were sampled between 10AM to 12PM. Sampled roots were immediately frozen into liquid nitrogen and ground using a TissueLyser II (Qiagen). RNA and cDNA (from 1µg of RNA) were prepared using extraction kits as described above. RT-PCR was performed with 1µL of diluted cDNA (1:9) in a Brillant III ultra fast SYBRgreen QPCR master mix (Agilent Technologies, USA) using a StepOnePlus Real-Time PCR System (Applied biosystems, USA). Primers used to amplify the different PgPIP genes were checked for specificity and efficiency prior to the experiment (S5 Table). The pearl millet Ubiquitin gene (*Pgl_GLEAN_10001684*) was used as reference and PgPIP relative expression was calculated according to the delta-delta ct method.

PgAQP expression in shoots were retrieved from [49]. Data from leaves and inflorescence of ten open pollinated cultivated pearl millet varieties were used [49].

Statistics

Statistical analyses were performed using R version 3.5.2 (R Development Core Team, 2018) using ANOVA (aov script) to detect significant differences. Least Significant Difference (LSD) test within the Agricolae package was used to group differences in letter classes.

Results

Pearl millet aquaporin contribution to root hydraulic conductivity

In order to evaluate if AQP function in root radial water flow could be associated with water use in pearl millet, we measured root hydraulic conductivity (Lpr) in IP4952 and IP17150,

previously described as low and high water use efficiency lines respectively. IP4952 showed 1.4 times higher Lpr than IP17150 (1.30E-07 ± 2.36E-08 versus 9.27E-08 ± 8.33E-09 m^3 m^{-2} s^{-1} MPa^{-1} respectively; n=15) but this difference was not significant (p = 0.148; Fig 1 and S1 Table). In both IP4952 and IP17150, treatment with azide, an inhibitor of AQP activity, led to significant Lpr reduction to 2.00E-08 ± 2.44E-09 and 2.19E-08 ± 2.32E-09 m^3 m^{-2} s^{-1} MPa^{-1} respectively (p < 0.001; S1 Table). This effect of azide application on Lpr was mostly reversible after treating the same roots with azide-free solution (S1 Fig). AQP contribution to Lpr was significantly higher in IP4952 (low water use efficiency) as compared to IP17150 (high water use efficiency; 84.64 ± 1.98% versus 76.40 ± 2.61%, p < 0.05; S1 Table). These data indicate that AQP could contribute more than 75% to Lpr in pearl millet.

Fig 1. Root hydraulic conductivity and aquaporin contribution in roots of IP4952 and IP17150. Root hydraulic conductivity (Lpr) were measured in plants grown in hydroponic conditions between 9AM to 12PM in presence or not of 2mM azide. (A) Lpr values measured in absence of azide. (B) Aquaporin contribution to Lpr was calculated as relative Lpr inhibition by azide. Bars represent mean values ± se of n=10-15 plants. *: p < 0.05.

Aquaporin identification and annotation

To have more insight in the AQP isoforms contributing to Lpr in pearl millet, we characterized the AQP genes family in the pearl millet genome. We blasted 772 AQP from the PIP, TIP, SIP, NIP and XIP families identified in 19 different species on the pearl millet reference genome (chromosome assembly and scaffolds) [43]. A total of 7005 sequences with bit score >100, representing 50 specific hits spread on the genome were identified (S2 Table). Forty-seven of the hits fall into previously annotated genes, one fall in a non-annotated part of the genome

on chromosome 5, and two in non-assembled parts of the genome (scaffold763 and scaffold8428).

Manual *de novo* annotation of the 50 putative AQP genes allowed the identification of eight genes with no start or with early stop codon in the first exon that were classified as pseudo-genes (S3 Table). Nine genes did not encode AQP isoforms but zinc-finger protein/LRR receptor-like serine-threonine protein kinase families or DEAD-like helicase-N superfamily, respectively. The absence of AQP signature domains (NPA and Ar/R motifs) in their protein sequence confirmed their non-affiliation to the AQP family. A number of genes showed an excessive number of exons or longer first exon and were re-annotated on the basis of alignment with transcriptome sequences or with close protein homologs (Uniprot/Swiss-Prot blast results) and presence of AQP isoform conserved domains. In addition, ten genes showed missing sequences in coding regions that were completed after sequencing. Overall, 33 *Pennisetum glaucum* AQP (PgAQP) genes were identified in the pearl millet genome, among which sixteen were *de novo* annotated (Table 1).

Table 1. Description and distribution of the aquaporins genes identified in pearl millet.

ID	Gene	Pgl_Glean ID	Gene length (bp)	Transcript length (bp)	Protein length (aa)	Protein MW (kD)	Chr	Start	End
Plasma membrane intrinsic proteins (PIP)									
1	*PgPIP1-1*	*Pgl_GLEAN_10001520*	3097	867	288	30.70	3	5721622	5724718
2	*PgPIP1-3*	*Pgl_GLEAN_10010809*	1601	867	288	30.76	3	274573998	274575598
3	*PgPIP1-4*	*Pgl_GLEAN_10005724*	992	900	298	31.38	2	104247932	104248932
4	*PgPIP2-1*	*Pgl_GLEAN_10028064*	2920	873	290	30.35	3	12453415	12456334
5	*PgPIP2-2*	*Pgl_GLEAN_10028876*	2830	867	288	30.12	3	45603209	45606038
6	*PgPIP2-3*	*Pgl_GLEAN_10035675*	1903	873	290	30.39	3	257669631	257671533
7	*PgPIP2-5*	*Pgl_GLEAN_10028056*	1062	834	277	28.93	3	12167791	12168852
8	*PgPIP2-6*	*Pgl_GLEAN_10028055*	1053	861	286	29.94	3	12156953	12158005
9	*PgPIP2-7*	*Pgl_GLEAN_10010255*	1170	861	286	29.79	Scaffold763	240584	241753
10	*PgPIP2-8*	*Pgl_GLEAN_10009812*	837	837	278	29.17	2	64966663	64967453
Tonoplast intrinsic proteins (TIP)									
11	*PgTIP1-1*	*Pgl_GLEAN_10002147*	1499	750	249	25.72	5	153303973	153305471
13	*PgTIP2-1*	*Pgl_GLEAN_10000631*	844	744	247	24.88	2	30657555	30658398
16	*PgTIP2-2*	*Pgl_GLEAN_10030617*	933	747	248	25.03	3	100540239	100541171
12	*PgTIP2-3*	*Pgl_GLEAN_10009584*	851	750	249	25.06	3	33622445	33623295
15	*PgTIP3-1*	*Pgl_GLEAN_10028702*	911	801	266	27.41	2	44624536	44625481
14	*PgTIP4-1*	*Pgl_GLEAN_10002901*	2586	738	245	25.58	1	263875434	263878070
18	*PgTIP4-2*	*Pgl_GLEAN_10003219*	1455	744	247	25.15	3	148813464	148814777
17	*PgTIP4-3*	*Pgl_GLEAN_10003218*	844	747	248	25.10	3	148807632	148808412
19	*PgTIP5-1*	*Pgl_GLEAN_10033583*	1087	813	270	26.69	3	272599938	272601028
Noduline-26 like intrinsic proteins (NIP)									
20	*PgNIP1-1*	*Pgl_GLEAN_10012175*	2316	846	281	29.52	2	195368171	195370486
21	*PgNIP1-2*	*Pgl_GLEAN_10028618*	2560	846	281	29.53	1	261387113	261389753
22	*PgNIP1-4*	*Pgl_GLEAN_10028339*	1137	837	278	29.36	3	145385690	145386826
23	*PgNIP2-1*	*Pgl_GLEAN_10018521*	3364	891	296	31.82	3	14105646	14109009
24	*PgNIP2-2*	*Pgl_GLEAN_10019286*	3821	894	297	31.57	2	103033018	103036838
25	*PgNIP3-1*	*Pgl_GLEAN_10034621*	3855	909	302	31.43	2	40497062	40500916
26	*PgNIP3-2*	*Pgl_GLEAN_10030882*	1151	846	281	29.60	4	55609410	55610656
27	*PgNIP3-3*	*Pgl_GLEAN_10030883*	1087	780	259	27.05	4	55648949	55650374
28	*PgNIP3-4*	*Pgl_GLEAN_10030881*	1258	750	249	25.15	4	55573901	55575272
29	*PgNIP3-5*	*Pgl_GLEAN_10030872*	934	837	278	27.79	4	55508562	55509419
30	*PgNIP4-1*	*Pgl_GLEAN_10012100*	1319	921	306	31.52	6	110090448	110091766
Small intrinsic proteins (SIP)									
31	*PgSIP1-1*	*Pgl_GLEAN_10003744*	2818	726	241	25.32	1	175152169	175154986
32	*PgSIP1-2*	*Pgl_GLEAN_10014008*	3375	759	252	25.91	4	93394125	93397493
33	*PgSIP2-1*	*Pgl_GLEAN_10026167*	1899	759	252	27.10	5	126489209	126491163

PgPIP2-7 is located on scaffold763 that was not assembled to the pearl millet genome. bp: base pairs; aa: amino-acids; MW: molecular weight; kD: kilo Dalton; Chr: chromosome; Start: position of the ATG; End: position of the stop codon.

Pearl millet aquaporins phylogenic analysis

To classify the PgAQP into families and name them, a phylogenetic tree was built using the PgAQP protein sequences along with protein sequences from *Arabidopsis thaliana*, *Oryza sativa* and *Populus tremula* (Fig 2). The PgAQP were named according to their grouping into families (PIP, TIP, SIP or NIP) and close homologs (Table 1). Ten isoforms showed homologies to the PIP family with three isoforms falling in the PIP1 sub-family (PgPIP1-1, PgPIP1-3 and PgPIP1-4) and seven isoforms falling in the PIP2 sub-family (PgPIP2-1, PgPIP2-2, PgPIP2-3,

PgPIP2-5, PgPIP2-6, PgPIP2-7 and PIP2-8). Nine isoforms from the *P. glaucum* TIP family (PgTIP), eleven isoforms from the *P. glaucum* NIP family (PgNIP) and three isoforms from the *P. glaucum* SIP family (PgSIP) were further identified. No isoforms from the XIP family were identified in pearl millet. This analysis further confirmed the classification of PgPIP1-1, PgPIP2-1, PgPIP2-3, PgPIP2-6, PgTIP1-1 and PgTIP2-2 cloned by [30]. However, PgPIP1-2 from [30] was renamed as PgPIP1-3 in this study.

PgAQP genes distribution in the pearl millet genome denoted that most of them were localized on chromosome 3 while none were localized on chromosome 7 (Fig 3). Two hot-spots of PgAQP genes were observed, one located in a region of 11899bp on chromosome 3 containing *PgPIP2-1*, *PgPIP2-5* and *PgPIP2-6* and the other in a region of 141812bp on chromosome 4 containing *PgNIP3-2*, *PgNIP3-3*, *PgNIP3-4* and *PgNIP3-5*.

Fig 2. Phylogenetic relationship among aquaporins isoforms from pearl millet, Arabidopsis, rice and poplar. Tree was generated using the Maximum Likelihood method with 1000 reiterations in MEGA7. Bootstrap values above 50% are represented. The PIP, TIP, SIP, NIP and XIP family clades are represented by blue, grey, purple, green and red, respectively. Pearl millet sequences are indicated by colored dots.

Fig 3. Distribution of aquaporin genes in the pearl millet genome. The seven chromosome (Chr) from the pearl millet genome are represented according to their size in megabase (Mb). Positions of PIP, TIP, SIP and NIP genes are represented in blue, purple, orange and green, respectively. *PgPIP2-7* which is located on scaffold763 is not represented.

Aquaporin gene structure in pearl millet

PgAQP genes showed large variation in gene length (ranging from 837bp for *PgPIP2-8* to 3855bp for *PgNIP3;1*; Table 1). Transcript length were less variable and relatively conserved within families with lengths of around 800-900bp for the PgPIP and PgNIP genes, 750-800bp for the PgTIP genes and 700-750bp for the PgSIP genes.

To investigate associations between phylogenetic classification and gene structure, the intron-exon organization of the PgAQP genes was analyzed (S2 Fig). PgAQP genes displayed between one (*PgPIP2-8*) to five exons (*PgNIP2-1*, *PgNIP2-2* and *PgNIP4-1*). Except for the NIP family, intron-exon organization was generally conserved within families with 5/9 PgPIP genes displaying 3 exons, 6/9 PgTIP genes displaying 2 exons and all PgSIP genes displaying 3 exons, supporting their phylogenetic distribution. *PgPIP2-5/PgPIP2-6* and *PgNIP3-2/PgNIP3-3* that were found to be close homologs in the phylogenetic analysis (Fig 2) and closely located in the pearl millet genome (Fig 3) showed similar gene and transcript length (Table 1) as well as gene structure (S2 Fig). PgAQP coding regions encoded proteins with length varying between 250 to 300 amino acids, with molecular weight of around 30kD for the PgPIP and PgNIP and 25kD for the PgTIP and PgSIP isoforms (Table 1).

Pearl millet AQP conserved domains

To investigate polymorphisms in the PgAQP isoforms conserved motifs that could underlay potential changes in structural and substrate selectivity, analyses of conserved and transmembrane domains were performed. The conserved domain analysis showed that all PgAQP isoforms belonged to the MIP super-family and displayed typical double NPA motifs (S6 Table and Table 2). Although some polymorphisms in the NPA motifs were observed in some isoforms (particularly from the NIP family) the subsequent amino-acids were of the same chemical properties (generally neutral and non-polar; Table 2, Fig 4 and S3-5 Fig). Ar/R

334 selectivity filters and Froger's residues known as AQP markers were well conserved in the
335 PgPIP isoforms except for the Froger's residue on position 1 (P1; Table 2, Fig 4). More
336 polymorphisms were observed in these residues for the PgTIP, PgNIP and PgSIP isoforms
337 although the ar/R residue on Loop E (R on LE2) and the Froger's residues at positions 3 (A) and
338 4 (F/Y) were well conserved across all isoforms (Table 2).

339 Transmembrane domains analyses using three different prediction softwares
340 suggested a high probability for all identified PgAQP to display six transmembrane domains
341 with cytoplasmic N-terminal and C-terminal ends as typically observed for AQP (S7 Table).
342 Predictions of the 3-dimensional geometry structure and pore morphology suggested a
343 continuous pore that runs longitudinally across both sides of the membranes for all PgPIP (S6
344 Fig). Two deviations in the pore center were typically observed at both extremities illustrating
345 the two constraints caused by the NPA motifs structured as alfa-helixes and acting as
346 selectivity filters.

347

348 **Fig 4. Conserved domains and membrane topology of the PIP isoforms from pearl millet.**
349 Alignment of the PIP isoforms were obtained using ClustalW in Mega7. Sequence identities
350 and similarities (80%) are highlighted in colors. The transmembrane domains are represented
351 by orange bars with the N-terminal and C-terminal ends of the protein located in the cytosol.
352 NPA: Asparagine-Proline-Alanine motifs; *: Aromatic/Arginine selectivity filters. #: Froger's
353 residues.

Table 2. Amino-acids residues in the conserved domains of the pearl millet aquaporins isoforms.

Isoform	NPA (LB)	NPA (LE)	Ar/R selectivity filters				Froger's residue				
			H2	H5	LE1	LE2	P1	P2	P3	P4	P5
Plasma membrane intrinsic proteins (PIP)											
PgPIP1-1	NPA	NPA	F	H	T	R	Q	S	A	F	W
PgPIP1-3	NPA	NPA	F	H	T	R	Q	S	A	F	W
PgPIP1-4	NPA	NPA	F	H	T	R	V	S	A	F	W
PgPIP2-1	NPA	NPA	F	H	T	R	Q	S	A	F	W
PgPIP2-2	NPA	NPA	F	H	T	R	Q	S	A	F	W
PgPIP2-3	NPA	NPA	F	H	T	R	Q	S	A	F	W
PgPIP2-5	NPA	NPA	F	H	T	R	-	S	A	F	W
PgPIP2-6	NPA	NPA	F	H	T	R	Q	S	A	F	W
PgPIP2-7	NPA	NPA	F	H	T	R	T	S	A	F	W
PgPIP2-8	NPA	NPA	F	H	T	R	H	S	A	F	W
Tonoplast intrinsic proteins (TIP)											
PgTIP1-1	NPA	NPA	H	I	A	V	T	S	A	Y	W
PgTIP2-1	NPA	TPA	H	I	G	R	T	S	A	Y	W
PgTIP2-2	NPA	NPA	H	I	G	R	T	S	A	Y	W
PgTIP2-3	NPA	NPA	H	I	G	R	T	S	A	Y	W
PgTIP3-1	NPA	NPA	H	V	A	R	T	V	A	Y	W
PgTIP4-1	NPS	NPA	N	S	A	R	T	S	A	Y	W
PgTIP4-2	NPA	NPA	Q	S	A	R	T	S	A	Y	W
PgTIP4-3	NPA	NPA	H	I	A	H	T	S	A	Y	W
PgTIP5-1	NPA	NPA	Q	V	A	R	R	S	A	Y	W
Noduline-26 like intrinsic proteins (NIP)											
PgNIP1-1	NPA	NPA	W	V	A	R	F	T	A	Y	V
PgNIP1-2	NPA	NPA	W	V	A	R	F	T	A	Y	F
PgNIP1-4	NPA	NPV	W	A	A	R	F	S	A	Y	I
PgNIP2-1	NPA	NPA	G	S	G	R	L	T	A	Y	F
PgNIP2-2	NPA	NPA	G	S	G	R	L	T	A	Y	F
PgNIP3-1	NPS	NPV	A	I	G	R	F	T	A	Y	L
PgNIP3-2	NPA	NPA	A	A	A	R	Y	T	A	Y	M
PgNIP3-3	NPA	NPA	A	A	A	R	Y	T	A	Y	M
PgNIP3-4	NPA	NPA	A	A	A	R	Y	T	A	Y	M
PgNIP3-5	NPA	NPA	A	A	A	R	Y	T	A	Y	M
PgNIP4-1	NPA	NPI	M	G	G	R	M	T	A	Y	L
Small intrinsic proteins (SIP)											
PgSIP1-1	NPT	NPA	V	V	P	N	M	A	A	Y	W
PgSIP1-2	NPT	NPA	L	I	P	N	M	A	A	Y	W
PgSIP2-1	NPL	NPA	S	H	G	S	F	A	A	Y	W

The two NPA (Asparagine-Proline-Alanine) motifs are located on loop B (LB) and loop E (LE). Aromatic/Arginine motifs (Ar/R) are located on helix 2 (H2), helix 5 (H5), and loop E (LE1 and LE2). P1-5 designed the five Froger's position.

Aquaporin expression profiling in pearl millet

Because of their localization at the plasma membrane, PIP isoforms play major roles in root hydraulic conductivity. To infer PgPIP isoforms putative importance to Lpr in pearl millet, we analyzed PgPIP gene expression pattern in roots of IP4952 and IP17150 using quantitative PCR.

PgPIP genes were generally more expressed in IP4952 as compared to IP17150 (Fig 5). In both lines, the most expressed genes in roots were *PgPIP1-1*, *PgPIP1-3*, *PgPIP1-4*, and *PgPIP2-3* while *PgPIP2-5*, *PgPIP2-6*, *PgPIP2-7* and *PgPIP2-8* were lowly expressed. *PgPIP1-3* and *PgPIP1-4* were the only genes significantly differentially expressed between both lines.

Expression of PgPIP in shoots (leaves and inflorescence) were retrieved from [49]. Transcriptomic analyses from ten pearl millet varieties suggest that *PgPIP1-4* and *PgPIP2-3*, two of the most expressed genes in roots, are lowly expressed in shoots (S7 Fig). Conversely, *PgPIP1-1* and *PgPIP1-3* are highly expressed in roots and shoots.

Fig 5. Relative expression of PIP genes in roots of IP4952 and IP17150. Transcript abundance of each PIP genes were measured between 9AM and 12PM on plants grown in hydroponic conditions and normalized to the expression of *PgPIP2-5* in IP4952. Bars show mean values ± se of n=6-8 biological replicates, each with technical triplicates. Letters indicate different significance groups.

Discussion

Here, we studied the role of AQP in root water transport in pearl millet, a heat and drought-adapted crop. Root hydraulic conductivity (Lpr) varied around 1E-07 m^3 m^{-2} s^{-1} MPa^{-1}, in a range that has been previously reported in other plants [54]. Root treatment with a common AQP inhibitor (azide) suggested that AQP contribute up to 84% to the Lpr in pearl millet (S1 Table). This figure is higher than what has been observed in Arabidopsis (57 to 64%) [55] and rice (42 to 79%) [56]. However, as complete reversion of Lpr inhibition by azide could be observed (S1 Fig), we do not think AQP contribution might have been over-estimated due to

387 azide secondary effects. Hence, our results suggest that PgAQP are major regulators of root
388 water flow in pearl millet.

389 We used the pearl millet genome sequence to characterize the AQP gene family and
390 identified thirty-three putatively functional AQP isoforms (based on conserved domains and
391 protein topology) that belonged to the PIP (10), TIP (9), SIP (3) and NIP (11) families. No XIP
392 were identified in pearl millet which confirm the absence of isoforms from this family in the
393 monocotyledon clade [8]. The number of identified AQP in pearl millet is similar to what has
394 been observed in *A. thaliana* (35) [57], rice (33) [22] and maize (31) [19]. Interestingly, AQP
395 genes were over-represented on Chromosome 3 with fourteen genes (Fig 3). *PgPIP2-5* and
396 *PgPIP2-6* closely located in Chromosome 3 are phylogenetically related and possess similar
397 gene structure (Fig 3 and S2 Fig) suggesting possible tandem duplication events in this region
398 [58]. Similarly, *PgNIP3-2* and *PgNIP3-3* located on Chromosome 4 may be the result of
399 duplication events. Furthermore, *PgPIP2-7* was identified in scaffold763 suggesting that genes
400 may be missing on parts of the pearl millet genome assembly.

401 The selectivity of plant AQP is defined by amino-acids structuring the pore that
402 constitute their signatures. Among these amino-acids, the NPA motifs on loops B and E
403 contribute with the dipole moment of the α-helices to prevent proton permeation [59,60].
404 These motifs were strictly conserved in the PgPIP but showed some polymorphisms for other
405 isoforms (Table 2). However, these substitutions did not drastically change the positive
406 electrostatic potential at the NPA motifs suggesting that proton exclusion from AQP pore is
407 conserved in pearl millet. Furthermore, the Ile preceding the Froger's residue P4 and P5 at the
408 end of Loop E, shown to be essential for CO_2 transport in PIP [61], is conserved in the PgPIP
409 (Fig 4).

The ar/R motifs, composed of four amino-acids forming a constriction at the extracytosolic entry of the pore, represent the main selectivity filter. Modelling approaches based on ar/R signatures were used to predict permeability of plant AQP [12,13]. For instance, the F-H-T-R signature observed in the PgPIP (Table 2) which seems strictly conserved across PIP from different species has been associated with water and H_2O_2 permeability [14,25,26,62]. The H-I-G-R signature observed in PgTIP2-1, PgTIP2-2 and PgTIP2-3 that is conserved in TIP2 from Arabidopsis, maize and rice supposedly allow permeability to water, NH_3, urea and H_2O_2 while the H-I-A-V signature observed in the unique PgTIP1 (PgTIP1-1) may allow NH_3, urea and H_2O_2 but restrict water permeation [63–65]. In PgNIP, the W-V-A-R signature have been associated with water, NH_3 and H_2O_2 transports while the A-I/A-G/A-R signatures were restricted to water and NH_3. Interestingly, PgNIP2-1 and PgNIP2-2 showed similar ar/R signature (G-S-G-R) than OsNIP2-1 that is permeable to silicon [18] and possess precise spacing of 108 amino-acids between the two NPA motifs supposed as essential for silicon permeability [66].

AQP in plants are expressed from root to leaf tissues, including inflorescence and pollen. Some PgPIP genes show tissue-specific expression with *PgPIP1-4* and *PgPIP2-3* being more specifically expressed in roots while *PgPIP2-1* is more specifically expressed in shoots and *PgPIP1-1* and *PgPIP1-3* are expressed in both tissues (Fig 5 and S7 Fig). It has been shown that PIP isoforms agglomerate as tetramers in the plasma membrane, each monomer forming functional units. Functional studies as well as protein-protein interactions studies suggest that PIP tetramers can be formed of heteromers of PIP1 and PIP2 with distinct functional properties depending on the isoform combination [67–70]. Based on PgPIP gene expression in pearl millet, PgPIP1-1, PgPIP1-3 and PgPIP1-4 might interact with PgPIP2-3 to form

433 heteromers in roots while PgPIP1-1, PgPIP1-3 and PgPIP2-1 might form different combinations
434 of heteromers in shoots.

435 Intraspecific diversity in AQP isoform expression have been observed in rice and
436 Arabidopsis [55,56,71,72]. In our study, diversity in expression pattern of PgAQP genes were
437 observed between two pearl millet inbred lines with different water use strategies (Fig 5).
438 IP4952 that showed significantly higher AQP contribution to Lpr as compared to IP17150 also
439 showed significantly higher *PgPIP1-3* and *PgPIP1-4* gene expression. These results suggest that
440 differences in expression of these AQP genes can reflect differences in AQP contribution to
441 Lpr in pearl millet. These observations are in line with results from [34] showing that the
442 expression of *VvPIP1-1* is associated to root hydraulics and response to water stress in two
443 isohydric and anisohydric grapevine (*Vitis vinifera*) cultivars. Transpiration response to high
444 VPD in four pearl millet recombinant inbred lines from a high resolution cross have been linked
445 to PgPIP gene expression in roots [30]. These authors suggested that a down-regulation of
446 PgPIP genes under high VPD induced reduction in transpiration and water savings. Our results
447 showing reduced expression of *PgPIP1-3* and *PgPIP1-4* and AQP contribution to Lpr in IP17150,
448 the line with higher water use efficiency, support the observations of [30]. Overall, expression
449 profiling suggests that APQ may have different physiological functions across the pearl millet
450 plant and contribute to its response to the environment. However, expression alone is
451 certainly not fully representative of AQP function due to the many post-translational
452 regulations affecting their activity [8]. Further investigations are needed to better understand
453 the links between reduction in transpiration under high VPD, improved water use efficiency
454 and AQP function in roots.

455 Pearl millet is a drought-adapted crop that will play a major role in the adaptation of
456 agriculture to future climate in arid and semi-arid regions of Africa and India. Here, we provide

a comprehensive view of the AQP genes and isoforms present in pearl millet as well as their contribution in root radial water transport. We confirmed the presence of selectivity filters suggesting permeability to water in the PgAQP and point isoforms PgPIP1-3 and PgPIP1-4 as potential main contributors of root water transport in pearl millet. The function of these isoforms may be subjected to natural diversity and associated with plant water use strategies as suggested by their differential expression in pearl millet lines contrasting for Lpr and water use efficiency. Therefore, our study supports a potential role for AQP in regulating pearl millet hydraulics and potentially adaptation to challenging environmental conditions.

Declaration of competing interest

No conflicts of interest declared

Acknowledgments

The authors are grateful to Dr Prakash Gangashetty (ICRISAT, Niger) for providing seeds of the inbred lines used in this study and Dr Kwanho Jeong (IRD, France) for his kind support in the preparation of this manuscript. The authors acknowledge the IRD iTrop HPC (South Green Platform) at IRD Montpellier for providing HPC resources that have contributed to the research results reported in this paper (https://bioinfo.ird.fr/- http://www.southgreen.fr).

Funding

This work was supported by the CGIAR Research Programme on Grain Legumes and Dryland Cereals (GLDC). PA was supported by the Cultivar program from the Agropolis Foundation as

479 part of the "Investissement d'Avenir" (ANR-l0-LABX-0001-0l) under the frame of I-SITE MUSE
480 (ANR-16-IDEX-0006). The French Agence Nationale de la Recherche supports the post-
481 doctoral fellowship of CFC (ANR Grant RootAdapt n°ANR17-CE20-0022-01 to LL).

482

483 Author contributions

484 AG, CTD and LL designed the study. AG, PA, CTD, CFC and CM performed the experiments. AG,
485 CTD, PA, CFC, CM, PG, VV, YV and LL analyzed the data and discussed the results. AG and LL
486 wrote the paper. All authors read and approved the manuscript.

487

References

1. Steudle E. The cohesion-tension mechanism and the acquisition of water by plant roots. Annu Rev Plant Physiol Plant Mol Biol. 2001;52: 847–875. doi:10.1146/annurev.arplant.52.1.847
2. Geldner N. The Endodermis. Annu Rev Plant Biol. 2013;64: 531–558. doi:10.1146/annurev-arplant-050312-120050
3. Wang P, Calvo-Polanco M, Reyt G, Barberon M, Champeyroux C, Santoni V, et al. Surveillance of cell wall diffusion barrier integrity modulates water and solute transport in plants. Sci Rep. 2019;9: 1–11. doi:10.1038/s41598-019-40588-5
4. Abascal F, Irisarri I, Zardoya R. Diversity and evolution of membrane intrinsic proteins. Biochim Biophys Acta. 2014;1840: 1468–1481. doi:10.1016/j.bbagen.2013.12.001
5. Verma RK, Gupta AB, Sankararamakrishnan R. Major intrinsic protein superfamily: Channels with unique structural features and diverse selectivity filters. Methods Enzymol. 1st ed. 2015;557: 485–520. doi:10.1016/bs.mie.2014.12.006
6. Froger A, Tallur B, Thomas D, Delamarche C. Prediction of functional residues in water channels and related proteins. Protein Sci. 1998;7: 1458–1468. doi:10.1002/pro.5560070623
7. Hub JS, De Groot BL. Mechanism of selectivity in aquaporins and aquaglyceroporins. Proc Natl Acad Sci U S A. 2008;105: 1198–1203. doi:10.1073/pnas.0707662104
8. Maurel C, Boursiac Y, Luu D-T, Santoni V, Shahzad Z, Verdoucq L. Aquaporins in plants. Physiol Rev. 2015;95: 1321–58. doi:10.1152/physrev.00008.2015
9. Ishikawa F, Suga S, Uemura T, Sato MH, Maeshima M. Novel type aquaporin SIPs are mainly localized to the ER membrane and show cell-specific expression in *Arabidopsis thaliana*. FEBS Lett. 2005;579: 5814–5820. doi:10.1016/j.febslet.2005.09.076
10. Wudick MM, Luu DT, Maurel C. A look inside: Localization patterns and functions of intracellular plant aquaporins. New Phytol. 2009;184: 289–302. doi:10.1111/j.1469-8137.2009.02985.x
11. Bienert GP, Bienert MD, Jahn TP, Boutry M, Chaumont F. *Solanaceae* XIPs are plasma membrane aquaporins that facilitate the transport of many uncharged substrates. Plant J. 2011;66: 306–317. doi:10.1111/j.1365-313X.2011.04496.x
12. Bansal A, Sankararamakrishnan R. Homology modeling of major intrinsic proteins in rice, maize and Arabidopsis: Comparative analysis of transmembrane helix association and aromatic/arginine selectivity filters. BMC Struct Biol. 2007;7: 1–17. doi:10.1186/1472-6807-7-27
13. Wallace IS, Roberts DM. Homology modeling of representative subfamilies of Arabidopsis major intrinsic proteins. Classification based on the aromatic/arginine selectivity filter. Plant Physiol. 2004;135: 1059–1068. doi:10.1104/pp.103.033415
14. Rodrigues O, Reshetnyak G, Grondin A, Saijo Y, Leonhardt N, Maurel C, et al. Aquaporins facilitate hydrogen peroxide entry into guard cells to mediate ABA- and pathogen-triggered stomatal closure. Proc Natl Acad Sci U S A. 2017;114. doi:10.1073/pnas.1704754114
15. Uehleln N, Lovisolo C, Siefritz F, Kaldenhoff R. The tobacco aquaporin NtAQP1 is a membrane CO_2 pore with physiological functions. Nature. 2003;425: 734–737. doi:10.1038/nature02027
16. Loqué D, Ludewig U, Yuan L, Von Wirén N. Tonoplast intrinsic proteins AtTIP2;1 and AtTIP2;3 facilitate NH_3 transport into the vacuole. Plant Physiol. 2005;137: 671–680.

534 doi:10.1104/pp.104.051268
535 17. Biela A, Grote K, Otto B, Hoth S, Hedrich R, Kaldenhoff R. The *Nicotiana tabacum*
536 plasma membrane aquaporin NtAQP1 is mercury-insensitive and permeable for
537 glycerol. Plant J. 1999;18: 565–570. doi:10.1046/j.1365-313X.1999.00474.x
538 18. Ma FJ, Kazunori T, Naoki Y, Namiki M, Saeko K, Maki K, et al. A silicon transporter in
539 rice. Nature. 2006;440: 688–691. doi:10.1038/nature04590
540 19. Chaumont F, Barrieu F, Wojcik E, Chrispeels MJ, Jung R. Aquaporins constitute a large
541 and highly divergent protein family in maize. Plant Physiol. 2001;125: 1206–1215.
542 doi:10.1104/pp.125.3.1206
543 20. Azad AK, Ahmed J, Md Asraful A, Md Mahbub H, Ishikawa T, Sawa Y, et al. Genome-
544 wide characterization of major intrinsic proteins in four grass plants and their non-
545 aqua transport selectivity profiles with comparative perspective. PLoS One. 2016;11:
546 e0157735. doi:10.1371/journal.pone.0157735
547 21. Reddy PS, Rao TSRB, Sharma KK, Vadez V. Genome-wide identification and
548 characterization of the aquaporin gene family in *Sorghum bicolor* (L.). Plant Gene.
549 2015;1: 18–28. doi:10.1016/j.plgene.2014.12.002
550 22. Sakurai J, Ishikawa F, Yamaguchi T, Uemura M, Maeshima M. Identification of 33 rice
551 aquaporin genes and analysis of their expression and function. Plant Cell Physiol.
552 2005;46: 1568–77. doi:10.1093/pcp/pci172
553 23. Guerriero G, Deshmukh R, Sonah H, Sergeant K, Hausman JF, Lentzen E, et al.
554 Identification of the aquaporin gene family in *Cannabis sativa* and evidence for the
555 accumulation of silicon in its tissues. Plant Sci. 2019;287: 110167.
556 doi:10.1016/j.plantsci.2019.110167
557 24. Reuscher S, Akiyama M, Mori C, Aoki K, Shibata D, Shiratake K. Genome-wide
558 identification and expression analysis of aquaporins in tomato. PLoS One. 2013;8:
559 e79052. doi:10.1371/journal.pone.0079052
560 25. Javot H, Lauvergeat V, Santoni V, Martin-Laurent F, Güçlü J, Vinh J, et al. Role of a
561 single aquaporin isoform in root water uptake. Plant Cell. 2003;15: 509–522.
562 doi:10.1105/tpc.008888
563 26. Postaire O, Tournaire-Roux C, Grondin A, Boursiac Y, Morillon R, Schäffner AR, et al. A
564 PIP1 aquaporin contributes to hydrostatic pressure-induced water transport in both
565 the root and rosette of Arabidopsis. Plant Physiol. 2010;152: 1418–1430.
566 doi:10.1104/pp.109.145326
567 27. Vadez V. Root hydraulics: The forgotten side of roots in drought adaptation. F Crop
568 Res. 2014;165: 15–24. doi:10.1016/j.fcr.2014.03.017
569 28. Moshelion M, Halperin O, Wallach R, Oren R, Way DA. Role of aquaporins in
570 determining transpiration and photosynthesis in water-stressed plants: Crop water-
571 use efficiency, growth and yield. Plant, Cell Environ. 2015;38: 1785–1793.
572 doi:10.1111/pce.12410
573 29. Shekoofa A, Sinclair T. Aquaporin activity to improve crop drought tolerance. Cells.
574 2018;7: 123. doi:10.3390/cells7090123
575 30. Reddy PS, Tharanya M, Sivasakthi K, Srikanth M, Hash CT, Kholova J, et al. Molecular
576 cloning and expression analysis of aquaporin genes in pearl millet [*Pennisetum*
577 *glaucum* (L) R. Br.] genotypes contrasting in their transpiration response to high
578 vapour pressure deficits. Plant Sci. 2017;265: 167–176.
579 doi:10.1016/j.plantsci.2017.10.005
580 31. Zhang C, Postma JA, York LM, Lynch JP. Root foraging elicits niche complementarity-

dependent yield advantage in the ancient ' three sisters ' (maize/bean/squash) polyculture. Ann Bot. 2014;114: 1719–1733. doi:10.1093/aob/mcu191

32. Tharanya M, Kholova J, Sivasakthi K, Seghal D, Hash CT, Raj B, et al. Quantitative trait loci (QTLs) for water use and crop production traits co-locate with major QTL for tolerance to water deficit in a fine-mapping population of pearl millet (*Pennisetum glaucum* L. R.Br.). Theor Appl Genet. 2018;131: 1509–1529. doi:10.1007/s00122-018-3094-6

33. Sadok W, Sinclair TR. Transpiration response of "slow-wilting" and commercial soybean (*Glycine max* (L.) Merr.) genotypes to three aquaporin inhibitors. J Exp Bot. 2010;61: 821–829. doi:10.1093/jxb/erp350

34. Vandeleur RK, Mayo G, Shelden MC, Gilliham M, Kaiser BN, Tyerman SD. The role of plasma membrane intrinsic protein aquaporins in water transport through roots: Diurnal and drought stress responses reveal different strategies between isohydric and anisohydric cultivars of grapevine. Plant Physiol. 2009;149: 445–460. doi:10.1104/pp.108.128645

35. Sakurai-Ishikawa J, Murai-Hatano M, Hayashi H, Ahamed A, Fukushi K, Matsumoto T, et al. Transpiration from shoots triggers diurnal changes in root aquaporin expression. Plant, Cell Environ. 2011;34: 1150–1163. doi:10.1111/j.1365-3040.2011.02313.x

36. Sade N, Vinocur BJ, Diber A, Shatil A, Ronen G, Nissan H, et al. Improving plant stress tolerance and yield production: Is the tonoplast aquaporin SiTIP2;2 a key to isohydric to anisohydric conversion? New Phytol. 2009;181: 651–661. doi:10.1111/j.1469-8137.2008.02689.x

37. Kholová J, Hash CT, Kakkera A, Koová M, Vadez V. Constitutive water-conserving mechanisms are correlated with the terminal drought tolerance of pearl millet [*Pennisetum glaucum* (L.) R. Br.]. J Exp Bot. 2010;61: 369–377. doi:10.1093/jxb/erp314

38. Kholová J, Nepolean T, Tom Hash C, Supriya A, Rajaram V, Senthilvel S, et al. Water saving traits co-map with a major terminal drought tolerance quantitative trait locus in pearl millet [*Pennisetum glaucum* (L.) R. Br.]. Mol Breed. 2012;30: 1337–1353. doi:10.1007/s11032-012-9720-0

39. Vadez V, Kholova J, Zaman-Allah M, Belko N. Water: The most important "molecular" component of water stress tolerance research. Funct Plant Biol. 2013;40: 1310–1322. doi:10.1071/FP13149

40. Debieu M, Kanfany G, Laplaze L. Pearl Millet Genome: Lessons from a Tough Crop. Trends Plant Sci. 2017;22: 911–913. doi:10.1016/j.tplants.2017.09.006

41. Sultan B, Defrance D, Iizumi T. Evidence of crop production losses in West Africa due to historical global warming in two crop models. Sci Rep. 2019;9: 1–15. doi:10.1038/s41598-019-49167-0

42. Debieu M, Sine B, Passot S, Grondin A, Akata E, Gangashetty P, et al. Response to early drought stress and identification of QTLs controlling biomass production under drought in pearl millet. PLoS One. 2018;13: 1–19. doi:10.1371/journal.pone.0201635

43. Varshney RK, Shi C, Thudi M, Mariac C, Wallace J, Qi P, et al. Pearl millet genome sequence provides a resource to improve agronomic traits in arid environments. Nat Biotechnol. 2017;35: 969–976. doi:10.1038/nbt.3943

44. Vadez V, Deshpande SP, Kholova J, Hammer GL, Borrell AK, Talwar HS, et al. Stay-green quantitative trait loci's effects on water extraction, transpiration efficiency and seed yield depend on recipient parent background. Funct Plant Biol. 2011;131: 1509–1529. doi:10.1071/FP11073

628 45. Vadez V, Kholova J, Medina S, Kakkera A, Anderberg H. Transpiration efficiency: New
629 insights into an old story. J Exp Bot. 2014;65: 6141–6153. doi:10.1093/jxb/eru040
630 46. Hoagland DR, Arnon DI. The water-culture method for growing plants without soil.
631 Calif Agr Expt Sta Circ. 1950;347: 1–32. doi:citeulike-article-id:9455435
632 47. Boursiac Y, Chen S, Luu D-T, Sorieul M, van den Dries N, Maurel C. Early effects of
633 salinity on water transport in Arabidopsis roots. Molecular and cellular features of
634 aquaporin expression. Plant Physiol. 2005;139: 790–805. doi:10.1104/pp.105.065029
635 48. Henry A, Cal AJ, Batoto TC, Torres RO, Serraj R. Root attributes affecting water uptake
636 of rice (*Oryza sativa*) under drought. J Exp Bot. 2012;63: 4751–4763.
637 doi:10.1093/jxb/ers150
638 49. Sarah G, Homa F, Pointet S, Contreras S, Sabot F, Nabholz B, et al. A large set of 26
639 new reference transcriptomes dedicated to comparative population genomics in
640 crops and wild relatives. Mol Ecol Resour. 2017;17: 565–580. doi:10.1111/1755-
641 0998.12587
642 50. Milne I, Stephen G, Bayer M, Cock PJA, Pritchard L, Cardle L, et al. Using tablet for
643 visual exploration of second-generation sequencing data. Brief Bioinform. 2013;14:
644 193–202. doi:10.1093/bib/bbs012
645 51. Hu B, Jin J, Guo AY, Zhang H, Luo J, Gao G. GSDS 2.0: An upgraded gene feature
646 visualization server. Bioinformatics. 2015;15: 1296–1297.
647 doi:10.1093/bioinformatics/btu817
648 52. Kelley LA, Mezulis S, Yates CM, Wass MN, Sternberg MJE. The Phyre2 web portal for
649 protein modeling, prediction and analysis. Nat Protoc. 2015;10: 845.
650 doi:10.1038/nprot.2015.053
651 53. Kumar S, Stecher G, Tamura K. MEGA7: Molecular Evolutionary Genetics Analysis
652 Version 7.0 for bigger datasets. Mol Biol Evol. 2016;33: 1870–1874.
653 doi:10.1093/molbev/msw054
654 54. Javot H, Maurel C. The role of aquaporins in root water uptake. Ann Bot. 2002;90:
655 301–313. doi:10.1093/aob/mcf199
656 55. Sutka M, Li G, Boudet J, Boursiac Y, Doumas P, Maurel C. Natural variation of root
657 hydraulics in Arabidopsis grown in normal and salt-stressed conditions. Plant Physiol.
658 2011;155: 1264–1276. doi:10.1104/pp.110.163113
659 56. Grondin A, Mauleon R, Vadez V, Henry A. Root aquaporins contribute to whole plant
660 water fluxes under drought stress in rice (*Oryza sativa* L.). Plant, Cell Environ. 2016;39.
661 doi:10.1111/pce.12616
662 57. Johanson U, Karlsson M, Johansson I, Gustavsson S, Sjövall S, Fraysse L, et al. The
663 complete set of genes encoding major intrinsic proteins in arabidopsis provides a
664 framework for a new nomenclature for major intrinsic proteins in plants. Plant
665 Physiol. 2001;126: 1358–1369. doi:10.1104/pp.126.4.1358
666 58. Tattini L, D'Aurizio R, Magi A. Detection of genomic structural variants from next-
667 generation sequencing data. Front Bioeng Biotechnol. 2015;25: 3–92.
668 doi:10.3389/fbioe.2015.00092
669 59. Chakrabarti N, Tajkhorshid E, Roux B, Pomès R. Molecular basis of proton blockage in
670 aquaporins. Structure. 2004;12: 65–74. doi:10.1016/j.str.2003.11.017
671 60. Törnroth-Horsefield S, Wang Y, Hedfalk K, Johanson U, Karlsson M, Tajkhorshid E, et
672 al. Structural mechanism of plant aquaporin gating. Nature. 2006;439: 688–694.
673 doi:10.1038/nature04316
674 61. Mori IC, Rhee J, Shibasaka M, Sasano S, Kaneko T, Horie T, et al. CO_2 transport by PIP2

aquaporins of barley. Plant Cell Physiol. 2014;55: 251–257. doi:10.1093/pcp/pcu003

62. Tournaire-Roux C, Sutka M, Javot H, Gout E, Gerbeau P, Luu D-T, et al. Cytosolic pH regulates root water transport during anoxic stress through gating of aquaporins. Nature. 2003;425: 393–397. doi:10.1038/nature01853

63. Maurel C, Reizer J, Schroeder JI, Chrispeels MJ. The vacuolar membrane protein gamma-TIP creates water specific channels in *Xenopus oocytes*. EMBO J. 1993;12: 2241–2247. doi:10.1002/j.1460-2075.1993.tb05877.x

64. Dynowski M, Schaaf G, Loque D, Moran O, Ludewig U. Plant plasma membrane water channels conduct the signalling molecule H_2O_2. Biochem J. 2008;414: 53–61. doi:10.1042/BJ20080287

65. Jahn TP, Møller ALB, Zeuthen T, Holm LM, Klærke DA, Mohsin B, et al. Aquaporin homologues in plants and mammals transport ammonia. FEBS Lett. 2004;574: 31–36. doi:10.1016/j.febslet.2004.08.004

66. Deshmukh RK, Vivancos J, Ramakrishnan G, Guérin V, Carpentier G, Sonah H, et al. A precise spacing between the NPA domains of aquaporins is essential for silicon permeability in plants. Plant J. 2015;83: 489–500. doi:10.1111/tpj.12904

67. Fetter K, Van Wilder V, Moshelion M, Chaumont F. Interactions between plasma membrane aquaporins modulate their water channel activity. Plant Cell. 2004;16: 215–228. doi:10.1105/tpc.017194

68. Zelazny E, Borst JW, Muylaert M, Batoko H, Hemminga MA, Chaumont F. FRET imaging in living maize cells reveals that plasma membrane aquaporins interact to regulate their subcellular localization. Proc Natl Acad Sci U S A. 2007;104: 12359–12364. doi:10.1073/pnas.0701180104

69. Yaneff A, Sigaut L, Marquez M, Alleva K, Pietrasanta LI, Amodeo G. Heteromerization of PIP aquaporins affects their intrinsic permeability. Proc Natl Acad Sci U S A. 2014;111: 231–236. doi:10.1073/pnas.1316537111

70. Bellati J, Alleva K, Soto G, Vitali V, Jozefkowicz C, Amodeo G. Intracellular pH sensing is altered by plasma membrane PIP aquaporin co-expression. Plant Mol Biol. 2010;74: 105–118. doi:10.1007/s11103-010-9658-8

71. Lian H-L, Yu X, Lane D, Sun W-N, Tang Z-C, Su W-A. Upland rice and lowland rice exhibited different PIP expression under water deficit and ABA treatment. Cell Res. 2006;16: 651–60. doi:10.1038/sj.cr.7310068

72. Alexandersson E, Danielson JÅH, Råde J, Moparthi VK, Fontes M, Kjellbom P, et al. Transcriptional regulation of aquaporins in accessions of Arabidopsis in response to drought stress. Plant J. 2010;61: 650–660. doi:10.1111/j.1365-313X.2009.04087.x

Supporting information

S1 Table. Root hydraulic conductivity (Lpr) and aquaporin (AQP) contribution in IP4952 and IP17150.

S2 Table. High scoring pairs with highest bit score at the fifty hot-spots.

S3 Table. Functional annotation of the pearl millet genomic regions corresponding to hotspots of High Scoring Pairs.

S4 Table. Primers used for genomic DNA (gDNA) or complementary DNA (cDNA) amplification of aquaporins showing missing sequence.

S5 Table. Primers used for quantitative RT-PCR.

S6 Table. Analysis of aquaporin conserved domains in pearl millet.

S7 Table. Transmembrane domain analysis of aquaporins in pearl millet.

S1 Fig. Reversion of azide-induced root hydraulic conductivity inhibition.

S2 Fig. Structure of pearl millet aquaporins genes.

S3 Fig. Conserved domains and membrane topology of the TIP isoforms from pearl millet.

S4 Fig. Conserved domains and membrane topology of the NIP isoforms from pearl millet.

S5 Fig. Conserved domains and membrane topology of the SIP isoforms from pearl millet.

S6 Fig. Cavity features of PgPIP isoforms.

S7 Fig. Expression pattern of PgPIP isoforms in shoots of pearl millet.

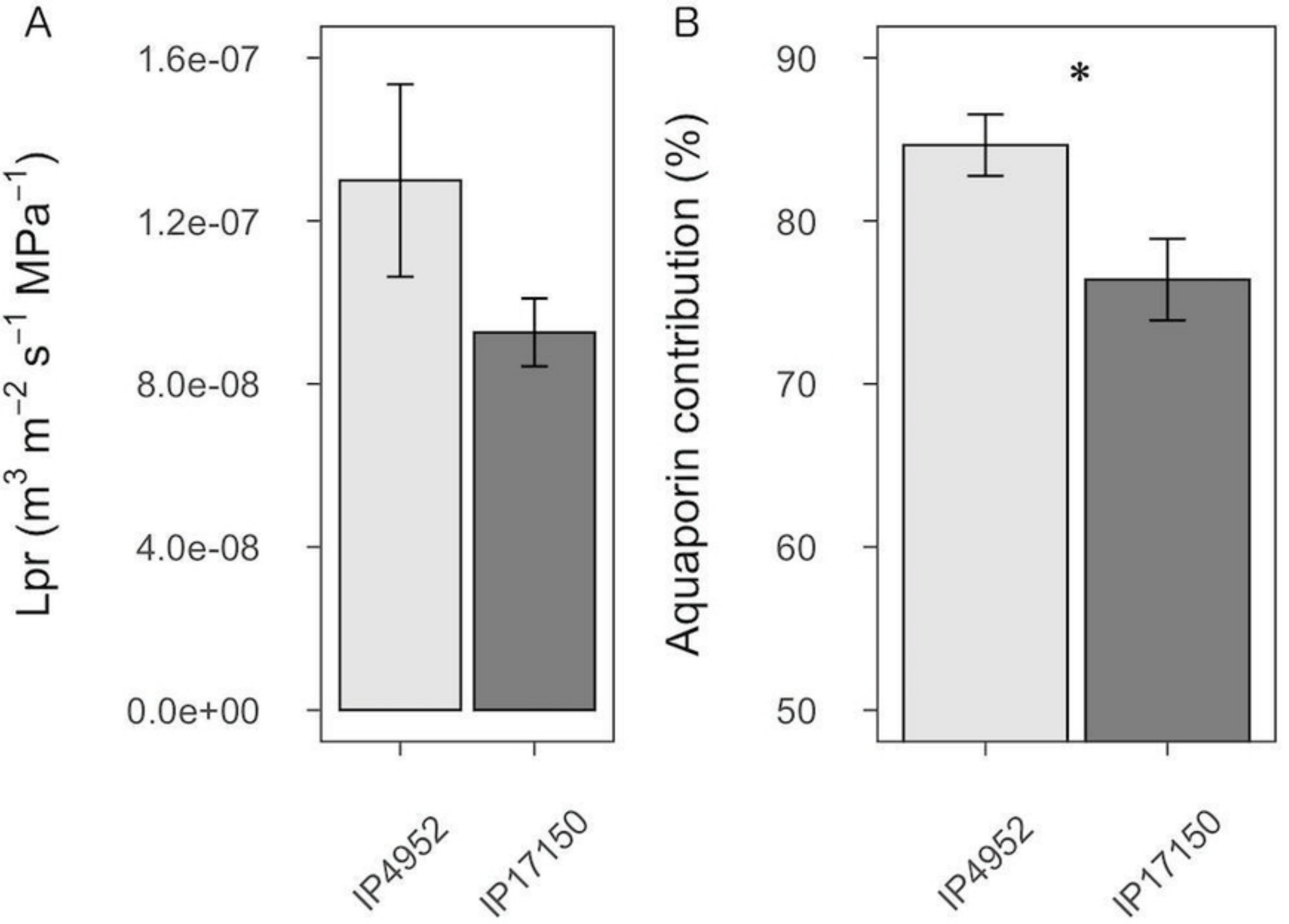
A
1.6e-07
1.2e-07
8.0e-08
4.0e-08
0.0e+00
Lpr (m3 m−2 s−1 MPa−1)
IP4952
IP17150
B
90
80
70
60
50
Aquaporin contribution (%)
*
IP4952
IP17150

Figure

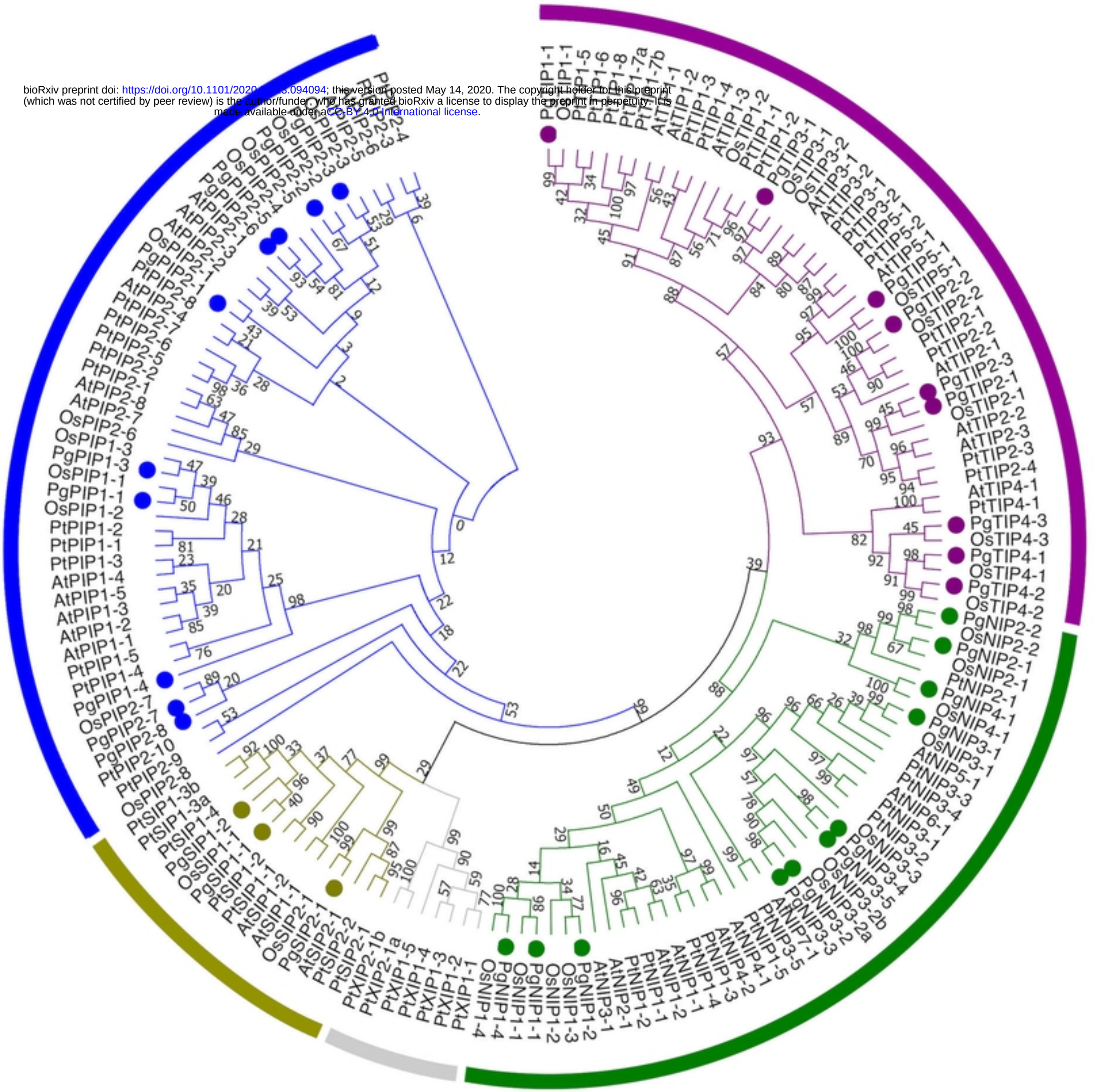

Figure

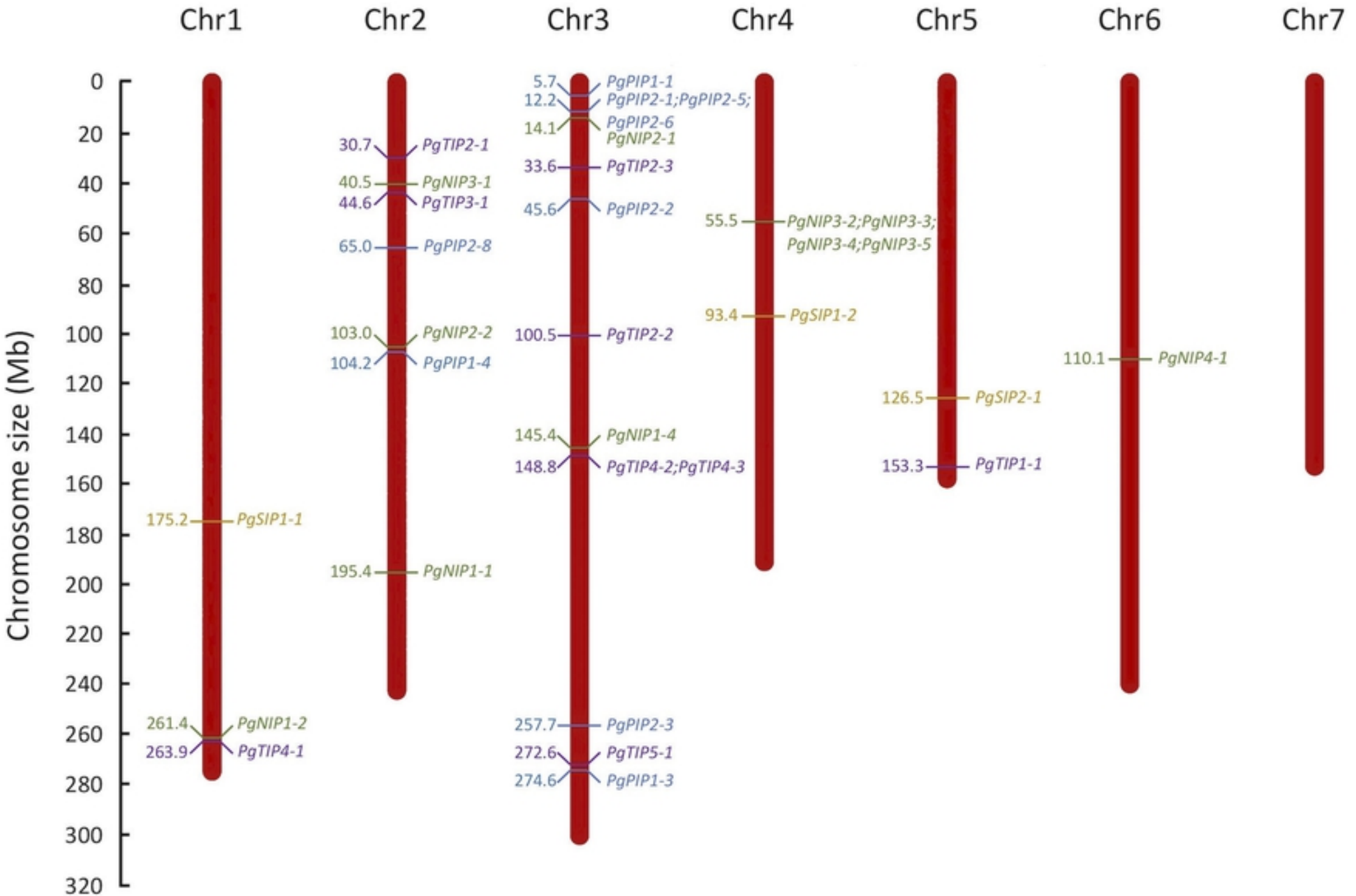
Chr1
Chr2
Chr3
Chr4
Chr5
Chr6
Chr7
Chromosome size (Mb)
0
20
40
60
80
100
120
140
160
180
200
220
240
260
280
300
320
175.2 PgSIP1-1
261.4 PgNIP1-2
263.9 PgTIP4-1
30.7 PgTIP2-1
40.5 PgNIP3-1
44.6 PgTIP3-1
65.0 PgPIP2-8
103.0 PgNIP2-2
104.2 PgPIP1-4
195.4 PgNIP1-1
5.7 PgPIP1-1
12.2 PgPIP2-1;PgPIP2-5;
14.1 PgPIP2-6
PgNIP2-1
33.6 PgTIP2-3
45.6 PgPIP2-2
100.5 PgTIP2-2
145.4 PgNIP1-4
148.8 PgTIP4-2;PgTIP4-3
257.7 PgPIP2-3
272.6 PgTIP5-1
274.6 PgPIP1-3
55.5 PgNIP3-2;PgNIP3-3;
PgNIP3-4;PgNIP3-5
93.4 PgSIP1-2
126.5 PgSIP2-1
153.3 PgTIP1-1
110.1 PgNIP4-1

Figure

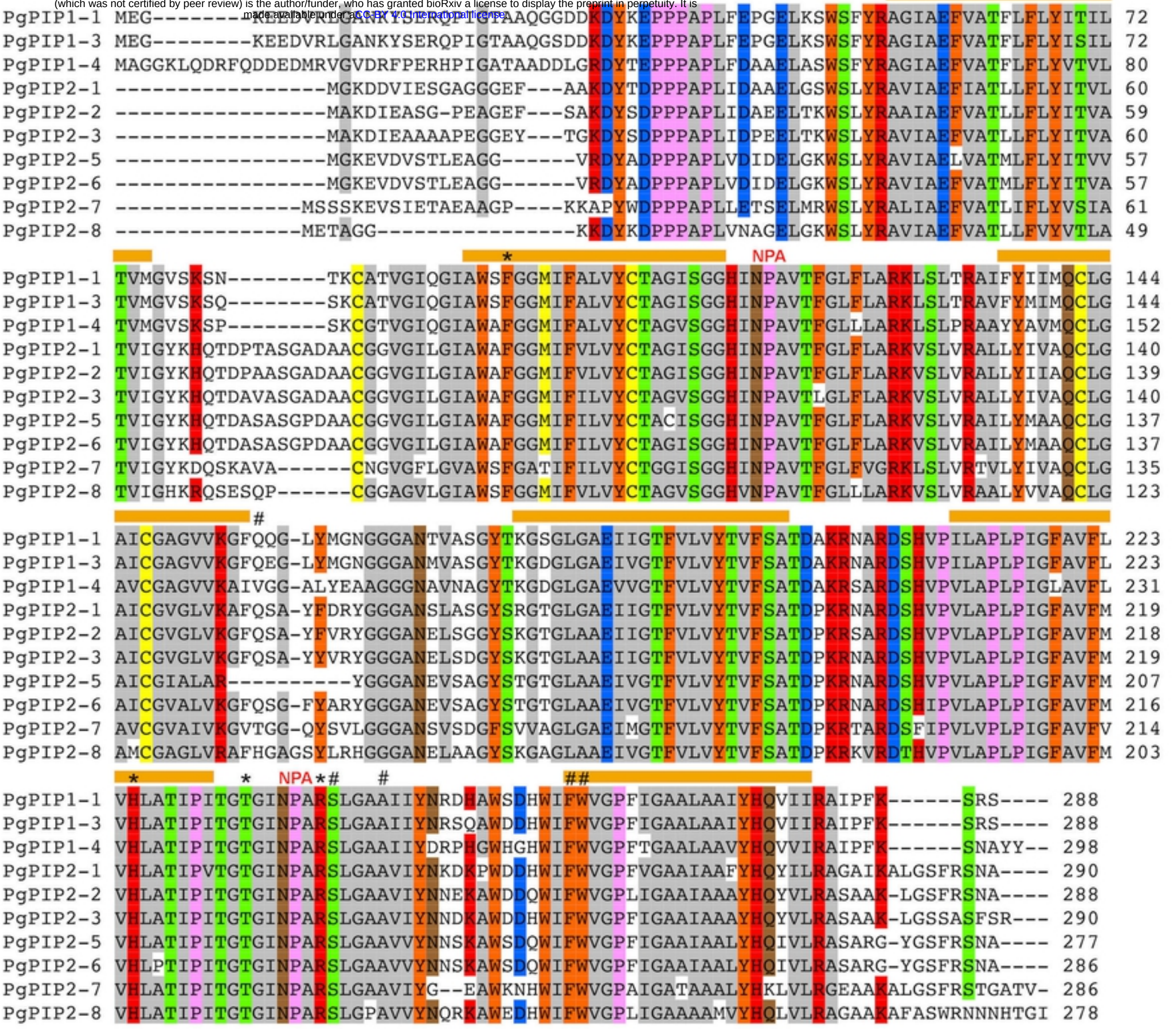

Figure

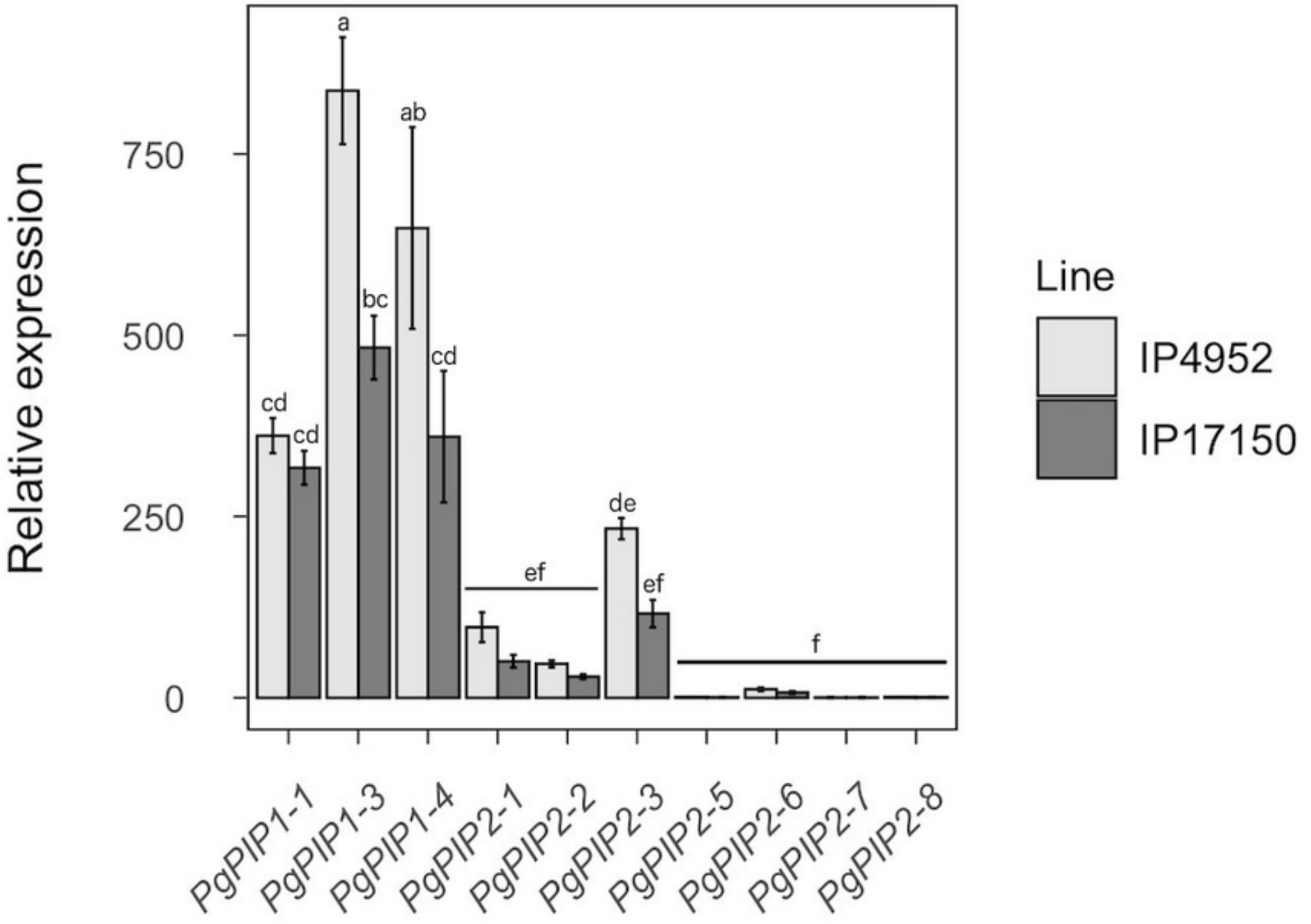
Relative expression
750
500
250
0
a
ab
bc
cd
cd
cd
cd
de
ef
ef
f
PgPIP1-1
PgPIP1-3
PgPIP1-4
PgPIP2-1
PgPIP2-2
PgPIP2-3
PgPIP2-5
PgPIP2-6
PgPIP2-7
PgPIP2-8
Line
IP4952
IP17150

Figure